Radiation Measurements 46 (2011) 860–865

Contents lists available at ScienceDirect

Radiation Measurements

journal homepage: www.elsevier.com/locate/radmeas

Dosimetry in the multi kilo-Gray range using optically-stimulated luminescence (OSL) and thermally-transferred OSL from quartz

C.I. Burbidge [a,b,*], S.I. Cabo Verde [a], A.C. Fernandes [a], M.I. Prudêncio [a,b], M.L. Botelho [a], M.I. Dias [a,b], G. Cardoso [a]

[a] Instituto Tecnológico e Nuclear, Sacavém, Portugal
[b] GEOBIOTEC, Universidade de Aveiro, Portugal

Keywords:
High dose retrospective dosimetry
Luminescence
LM-TT-OSL
Quartz

A B S T R A C T

This study explores the potential for using photon-stimulated luminescence of quartz grains to retrospectively evaluate multi-kGy gamma radiation doses. Subsamples from two ceramic tiles were given ^{60}Co gamma doses of 1, 3, 5, 15 and 30 kGy (nominal), accompanied by PMMA dosimeters and quartz grains from a geological sample known to exhibit thermally-transferred optically-stimulated luminescence (TTOSL). Following gamma irradiation, quartz grains were prepared from each subsample. OSL and TTOSL signals were measured for different preheat temperatures, and following re-irradiation with beta doses designed to equal the nominal gamma doses. OSL responses to 10 Gy beta test doses were measured following each cycle of high dose irradiation. Gamma doses were predicted from the beta responses, to evaluate the effectiveness of retrospective dose evaluation for different signal integrals, preheat combinations, and dose intervals. The use of linear modulation limited maximum OSL signal levels to 1.5×10^6 cps without reducing detector sensitivity, for the measurement of smaller TTOSL signals. The dosimetric behaviour of the three samples differed significantly: the best results were obtained from the pre-prepared geological quartz. OSL signals evident at short stimulation times, which are conventionally used for dosimetry and dating, did not in general appear appropriate for dosimetry in the range of doses examined. They exhibited dose response characteristics that were highly preheat dependant and variable in form between samples, which contained rapidly saturating and/or non-monotonic components. Higher preheats, up to 300 °C, preferentially removed OSL and TTOSL signals evident at longer stimulation times: those that remained yielded growth in signal with dose to approximately 10 kGy, but the accuracy of retrospective dose determinations was variable. TTOSL signals evident at short stimulation times increased proportionally with dose when 300 °C preheats were used, up to 30 kGy of beta irradiation for two of the samples, but the given gamma doses were underestimated by 15–23%. Refinement of the present measurement protocol may improve assessment of the gamma doses, and the short term stability of the signal needs to be characterised, but the observed level of accuracy is already sufficient to provide approximate estimates for severity of radiation exposure. The present study has identified certain elements of OSL and TTOSL signals that can be used, in combination with a relatively severe preheating regime, to retrospectively evaluate doses of tens of kGy: beyond the range traditionally possible using quartz.

1. Introduction

Thermoluminescence (TL) and photon- (or optically-) stimulated luminescence (PSL/OSL) of silicate minerals has been used for detection of multi-kGy irradiations for hygienisation and sterilisation for two decades (Sanderson et al., 1989). Luminescence methods are not generally used to quantitatively assess such large doses (1–50 kGy) because the signals commonly measured are thought to saturate, so that no correlation exists between luminescence signal and dose. However, certain types of luminescence signal have been shown to exhibit continued increases with dose through this range (Rink, 1994; Han et al., 2001). D'Oca et al. (2007) used multiple aliquot additive dose thermoluminescence (MAAD-TL) measurements to quantify 0.5 and 1 kGy doses in silicates separated from irradiated herbs. Carmichael and Sanderson used single aliquot regenerative thermoluminescence (SAR-TL) measurements to quantify 1–3 kGy doses in silicates separated from pasta: increases in signal with dose were evident up to 10 kGy (Sanderson, pers. comm.). Some types of OSL signal have been found to exhibit increases with laboratory beta

* Corresponding author. Instituto Tecnológico e Nuclear, Sacavém, Portugal.
E-mail address: christoph@itn.pt (C.I. Burbidge).

1350-4487/$ – see front matter © 2011 Elsevier Ltd. All rights reserved.
doi:10.1016/j.radmeas.2011.05.010

irradiation to a few kGy (Singarayer and Bailey, 2003). These signals derive from trapped charge populations with relatively low probabilities of detrapping per incident photon, i.e. they are relatively insensitive to light exposure and are hence evident at longer optical stimulation times. Thermally-transferred but photon-stimulated luminescence signals (TTOSL) have been found to exhibit increases to tens of kGy (Tsukamoto et al., 2008).

The TTOSL signal arises through the thermal transfer of charges between trap types in the band gap of the crystal. The source traps are emptied of charge by rapid heating to a given temperature, but are relatively insensitive to detrapping by photons of visible wavelengths. A small proportion of the charges liberated by heating are retrapped in photo-sensitive sites. In order to better observe the thermally-transferred signal, the photo-sensitive traps are first emptied by OSL measurement. The sample is then heated and the OSL measurement repeated to obtain the TTOSL. If it is desired to transfer charge from a restricted temperature interval, then the sample is heated prior to the initial OSL measurement, and then heated again to a higher temperature prior to TTOSL measurement. The measured TTOSL signal is thus expected to arise from thermally stimulable traps in the interval between the two "preheat" temperatures. The source of the TTOSL signal, as originally proposed, is thermally stimulable by heating to around 280 °C at 5 °C s^{-1} (Li and Li, 2006). The mean thermal lifetime of charge retention in the "280 °C TL" trap of quartz has been estimated to be 130–160 ka at 20 °C (Aitken, 1985; Spooner and Questiaux, 2000). A TTOSL signal derived from this temperature region may not be sufficiently stable for geological dating. However, the dose response characteristics noted above may make it suitable for retrospective dosimetry of multi-kGy radiation exposures, such as those employed for hygienisation and sterilisation.

The aim of the present study was to investigate the potential use of quartz in the evaluation of multi-kGy radiation doses, for retrospective dosimetry of subsamples from historic ceramic tiles irradiated for the purposes of biodecontamination. The objective was to identify OSL and TTOSL signals that continue to increase to multi-kGy doses, and test the utility of their regenerated responses for the accurate prediction of previously delivered gamma irradiations. The behaviours of different signal components were studied for a range of preheating conditions, to identify the combination that would provide the most accurate retrospective dose assessments.

2. Samples and methods

Two degraded 18th Century ceramic tiles were analysed ("Ceramic A", "Ceramic B"). Ceramic A consisted of a compact low-fired terracotta fabric, which had flaked as a result of fungal and bacterial infestation associated with wetting. Ceramic B had a coarse white high-fired fabric. It had suffered superficial discolouration due to colonisation by bacteria transferred from humans. Pre-prepared 160–250 μm quartz grains from a sample of Mozambican dune sand ("BZ05", Burbidge et al., 2009) were also analysed, since they were known to exhibit a TTOSL signal.

The samples were divided into six subsamples each. The quartz grains of BZ05 were annealed (300 °C/10 min) to reset the TTOSL signal associated with the 280 °C TL region, then loaded into six lightproof quartz pots (wall thickness 2 mm). The ceramics were broken into pieces but otherwise not processed, to simulate in situ irradiation of whole tiles. Environmental doses accumulated in the tiles since their manufacture were assumed to be approximately 1 Gy, and hence insignificant relative to the doses of interest to the present study.

The subsamples were first irradiated with nominal gamma doses of 0, 1, 3, 5, 15 and 30 kGy. The six quartz pots containing the prepared quartz grains, the six subsamples of each tile for luminescence testing, plus six other subsamples of each tile for microbiological analyses, were mounted in a single layer (~1 cm thick) in the centre of one face of a ceramic tile (15 × 15 × 0.5 cm). No sample was placed closer than 3 cm to the tile's edges. Harwell Red, Amber and Gammachrome PMMA dosimeters were placed above and below the samples to check the doses delivered to the samples, and a second ceramic tile fixed above. The outer ceramic tiles were designed to establish charged particle equilibrium for the samples, when the face of either tile was presented normal to the gamma irradiator.

Gamma irradiation was performed using the 250 kCi ^{60}Co multi-element source at the Centro de Higienização por Ionização de Produtos, S.A. (CHIP, ITN Campus). The sample assembly was irradiated 6 cm from the source (sample centres at 7 cm), in a region of approximately planar field. Dose rate to unshielded PMMA dosimeters in this geometry was estimated to be 12.4 ± 0.2 kGy h^{-1}, decay corrected from Portugal et al. (2010; 28–29 kGy h^{-1}, datum January 2004). This was confirmed with the PMMA dosimeters used in the present study, allowing for attenuation in the irradiation geometry and absorption by the samples at the average ^{60}Co gamma emission energy (1253 keV; Storm and Israel, 1970). Similarly, the dose rate to quartz in the centre of each sample was estimated to be 10.2 kGy h^{-1}. The different subsamples were irradiated for 5, 13, 21, 63, and 125 min (doses in Table 1, Step i).

Following gamma irradiation, quartz grains were prepared from the ceramic subsamples by disaggregation, sieving (90–250 μm) and acid treatment with HCl and HF (40% 40 min). Aliquots of quartz grains, both freshly prepared from the ceramics and pre-prepared from the pots, were deposited as monolayers on stainless steel cups for luminescence measurements and beta irradiations. For Ceramics A and B, the β Doses (Table 1, Step x) were delivered using a Daybreak 801E Beta Irradiator with a ^{90}Sr/^{90}Y source calibrated to deliver 0.18 Gy s^{-1} to the quartz grains in monolayers on stainless steel cups. Luminescence measurements (Table 1), preheats and other beta irradiations were conducted in a Risø DA-20 reader, with a ^{90}Sr/^{90}Y source calibrated to deliver 0.11 Gy s^{-1} to quartz grains in monolayers on stainless steel cups. OSL and TTOSL signals were stimulated using LEDs (470 nm), and detected through a U340 filter (50% T_{max} 280–370 nm) with the sample held at 125 °C. Ramping of power to the LEDs was used in all measurements: the resultant signal has been termed "linearly modulated OSL" or "LMOSL", and hence "TT-LM-OSL". In the present study all measurements were made using linear modulation, so the LM addition to the acronyms has only been used where pertinent.

Instrumental background was assessed by making LMOSL measurements on aliquots of annealed quartz, in the same experimental configuration as the dosimetric measurements (Fig. 1). This background was subtracted from the raw LMOSL signals. The LMOSL curves were then transformed into the shape that would have been produced by optical stimulation at a fixed power, based on Bulur (2000). This transformation produced conventional looking quartz OSL "decay curves", which were analysed using count rates derived from signals integrated over different stimulation time periods: 0–10 s, 0–100 s, and 100–400 s. The count rate in the period 400–500 s was subtracted from these to remove the effects of the components least sensitive to optical stimulation, which were assumed to be insignificantly depleted during the period of measurement.

A two-cycle "single aliquot regenerative" (SAR) sequence was applied (Table 1) to 30 aliquots per sample (24 for BZ05): 5 aliquots (4 for BZ05) were prepared for each of the 6 subsamples (dose levels), and each aliquot from a given subsample was measured using a different pair of preheat temperatures for OSL and TTOSL. Less thermally stable signal components induced by gamma irradiation were first removed by preheating (Table 1, Step ii), and the OSL signal measured (Step iii). A second preheat, 20 °C higher than the first, was

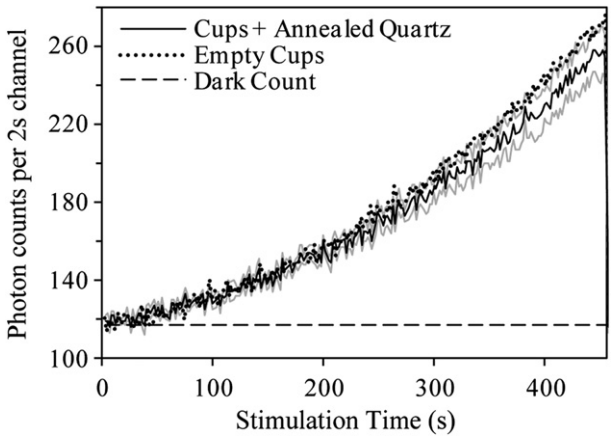

Fig. 1. LMOSL background. Means of 6 repeated measurements on 6 aliquots of pre annealed quartz (BZ05; 800 °C, cooled overnight) and 6 empty stainless steel cups. Results from repeated measurements were similar, but varied between cups. Empty and loaded cups yielded similar mean curves: the observed difference was approximately 1 sd.$n^{-½}$ (shown for the quartz aliquots as grey lines). Dark Count is the average of 40 s measurements following each of the LMOSL measurements. After subtraction of the average dark count, the curves were well approximated by the relationship $(cts/cts_{Max}) = (p/p_{Max})^a$, where LED power (p) is proportional to stimulation time: in this case a = 1.67. The values "Cups + Annealed Quartz" were subtracted from all dosimetric LMOSL measurements prior to their transformation.

then applied and the resultant TTOSL signal measured (Steps iv and v). A relatively small beta test dose was then administered (Step vi), and the OSL signal measured to monitor the sensitivity of each aliquot (Step viii). Following this, a rapid anneal to 500 °C was used to empty the dosimetry traps in the quartz (Step ix). Each aliquot was then beta irradiated with a similar dose to its nominal gamma dose (Step x), and the measurement process repeated (Steps xi-xviii). This sequence was designed to allow normalisation of signals produced by the large gamma and beta doses using those from the subsequent beta test doses, and hence to permit comparison between the dose responses of different aliquots with different sensitivities.

The resultant "dose-normalised multiple aliquot regenerative" dose response characteristics were fitted, with dose-normalised signal on the y axis and dose on the x axis, using linear regressions ($y = y_0 + Ax$) or saturating exponential curves of up to 5 parameters (Eqn. 1).

$$y = y_0 + A_1\left(1 - \exp^{-x/B_1}\right) + A_2\left(1 - e^{-x/B_2}\right) \quad (1)$$

For each equation, y-values were calculated for a range of incrementally spaced x-values ($x_n = 1.1^{(n-1)}$). The y-values calculated from the fits to the gamma dose response characteristics were each interpolated through the series of x:y pairs calculated from the fits to the corresponding beta dose response characteristics, to predict the x-values associated with them. This produced retrospective estimates of the doses absorbed during gamma irradiation, based on the beta dose response characteristics. The difference between each actual (gamma) and predicted (beta) x-value was then calculated for y-values (gamma) in the range in which signal continued to increase with dose. The size of these differences and their patterns of change

Table 1
Luminescence measurement sequence. Steps i-ix = gamma dose response. Steps x-xiii = beta dose response. Identification of the signal being measured at each stage is made in the Description column, i.e. "standard" OSL signals or "thermally-transferred" TTOSL signals. Both OSL and TTOSL were measured using linear modulation (LMOSL); 0–100% stimulation power ramped at 0.2% s^{-1} while held at 125 °C. The different doses given to each subsample, and the different pairs of preheats applied to each aliquot from each subsample, are indicated in the Details section.

Step	Description	Details						
i	*Subsample:*	*A*	*B*	*C*	*D*	*E*	*F*	*(all aliquots)*
	γ Dose	0	0.8	2.2	3.6	11	21	kGy
ii	*Aliquot:*	*1*	*2*	*3*	*4*	*5*		*(all subsamples)*
	Preheat	180	220	240	260	280		°C for 30 s
iii	OSL	"L1"						
iv	*Aliquot:*	*1*	*2*	*3*	*4*	*5*		*(all subsamples)*
	Preheat	200	240	260	280	300		°C for 30 s
v	TTOSL	"TTL1"						
vi	Test Dose	10 Gy β						
vii	Preheat	160 °C for 30 s						
viii	OSL	"T1"						
ix	Anneal	room temperature to 500 °C at 5 °C s^{-1}						
x	*Subsample:*	*A*	*B*	*C*	*D*	*E*	*F*	*(all aliquots)*
	β Dose	0.1	1	3	5	15	30	kGy
xi	*Aliquot:*	*1*	*2*	*3*	*4*	*5*		*(all subsamples)*
	Preheat	180	220	240	260	280		°C for 30 s
xii	OSL	"L2"						
xiii	*Aliquot:*	*1*	*2*	*3*	*4*	*5*		*(all subsamples)*
	Preheat	200	240	260	280	300		°C for 30 s
xiv	TTOSL	"TTL2"						
xv	Test Dose	10 Gy β						
xvi	Preheat	160 °C for 30 s						
xvii	OSL	"T2"						
xviii	Anneal	room temperature to 500 °C at 5 °C s^{-1}						

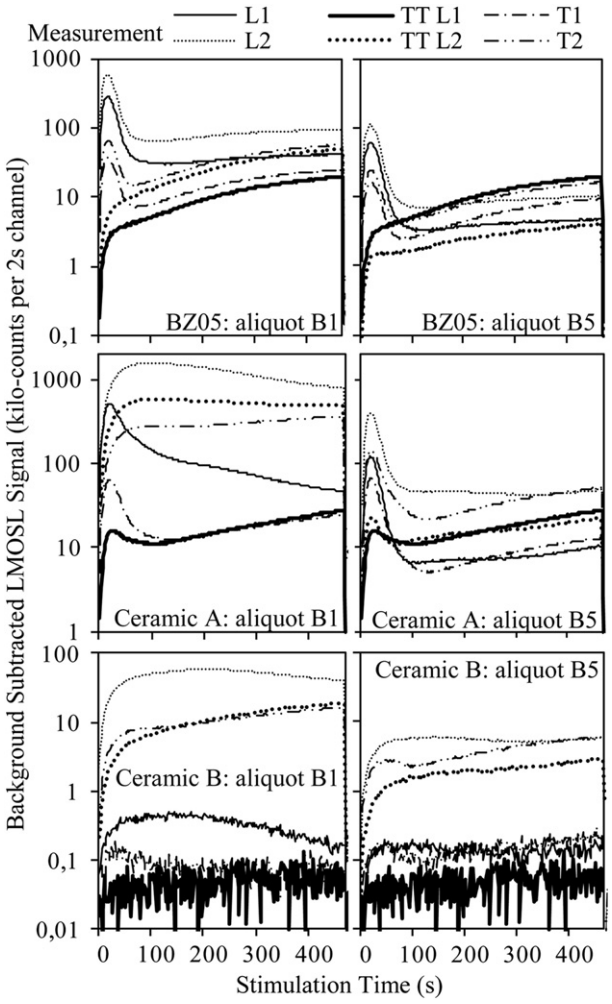

Fig. 2. LMOSL curves measured at each stage of the sequence (Table 1). Results are presented for aliquots 1 and 5 (mild or severe preheats) from subsample B (1 kGy) of each of the three samples BZ05, Ceramic A and Ceramic B. Measurements L1 and TTL1 = OSL and TTOSL responses to Gamma Dose (Table 1, Steps i, iii and v), L2 and TTL2 = OSL and TTOSL responses to Beta Dose (Table 1, Steps x, xii and xiv), T1 and T2 = OSL responses to 10 Gy beta Test Doses (Table 1, Steps vi, viii, xv xvii) to monitor changes in sensitivity from the Gamma cycle to the Beta cycle.

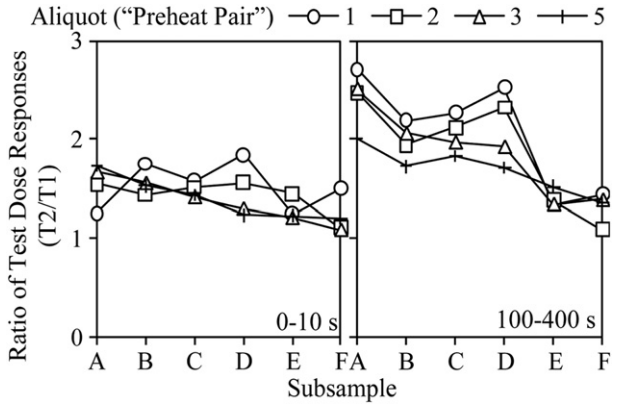

Fig. 3. Change in OSL sensitivity of sample BZ05 from one measurement cycle to the next (T2/T1; Table 1, Steps viii and xvii). The OSL signals were transformed from LMOSL measurements and integrated over different periods of optical stimulation (0–10 s, 100–400 s). Prior to irradiation with a test dose of 10 Gy, the response of each subsample (A–F) to a different dose of gamma or beta radiation (Table 1, Steps i, ×) had been measured following preheats of different severities (aliquot 1–5; Table 1, Steps ii, iv, xi, xiii. "Preheat Pair" 4 was not measured for sample BZ05). All aliquots were annealed to 500 °C between the gamma and beta cycles (Table 1, Step xvii).

with dose were used to evaluate the most useful combination of signal, preheat and dose range for accurate retrospective dosimetry.

3. Results

The LMOSL background increased as a power function of the voltage to the LEDs used for optical stimulation (Fig. 1). It was two to three orders of magnitude smaller than the majority of signals measured in the present study (Fig. 2).

OSL curves measured using linear modulation following irradiation to 1 kGy (Fig. 2), contained an initial rise through the first 10 s of stimulation or an initial peak in the first 100 s (henceforth termed "faster signals"). Signals evident at longer stimulation times exhibited rises and decays (100–400 s, henceforth termed "slower signals"). The maximum recorded count rate was 1.5×10^6 cps (Ceramic A, Subsample 5, Aliquot 1, Step xii). High preheats reduced signal levels at all stimulation times, but slower signals tended to be reduced more than faster ones. At higher doses the slower signals came to dominate the LMOSL curves.

Sensitivity increased from one measurement cycle to the next (e.g. Fig. 3 and compare curves L1, TTL1, T1 with L2, TTL2, T2 in Fig. 2). The magnitude of the increase varied strongly between the three samples, but in each case was smaller for the faster signals and following the higher preheats, where it was approximately 1.5 times for BZ05 and Ceramic A. Ceramic B initially had very low sensitivity but exhibited much stronger sensitisation; around 80 times at lower doses (Fig. 2, signals T1, T2) and around 15 times for higher doses and preheats.

Integrals of faster or slower signals from the transformed luminescence data are presented in Fig. 4, for aliquots 1 and 5 of each subsample (A-F) of sample BZ05. Inter-aliquot variation in sensitivity was evident in both test dose response (T#) and dose response (L#; TTL#). At higher doses the faster OSL signals varied mainly as a function of sensitivity. The slower OSL signals continued to increase gradually with dose at higher doses (Fig. 4): at a similar

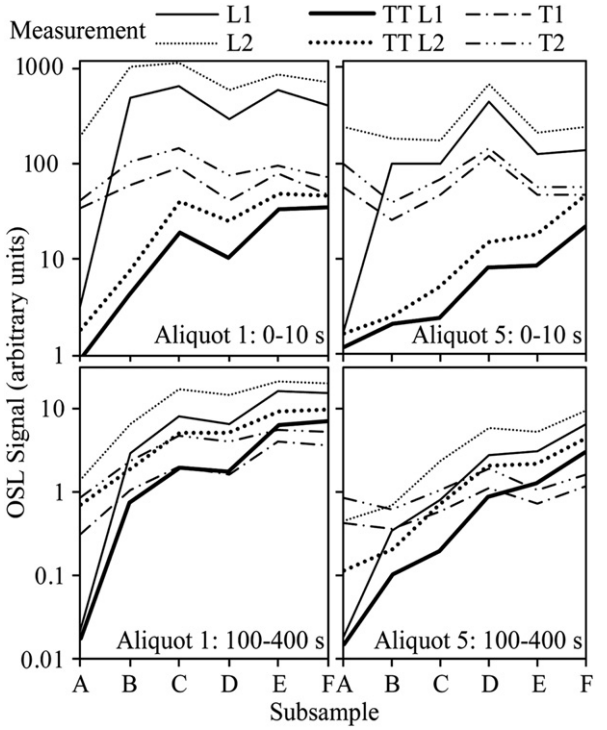

Fig. 4. OSL signals measured from sample BZ05 at each stage of the sequence (Table 1). Data are presented for aliquots 1 and 5 (mild or severe preheats) taken from each subsample A to F (different gamma and beta doses). And see Fig. 3 caption.

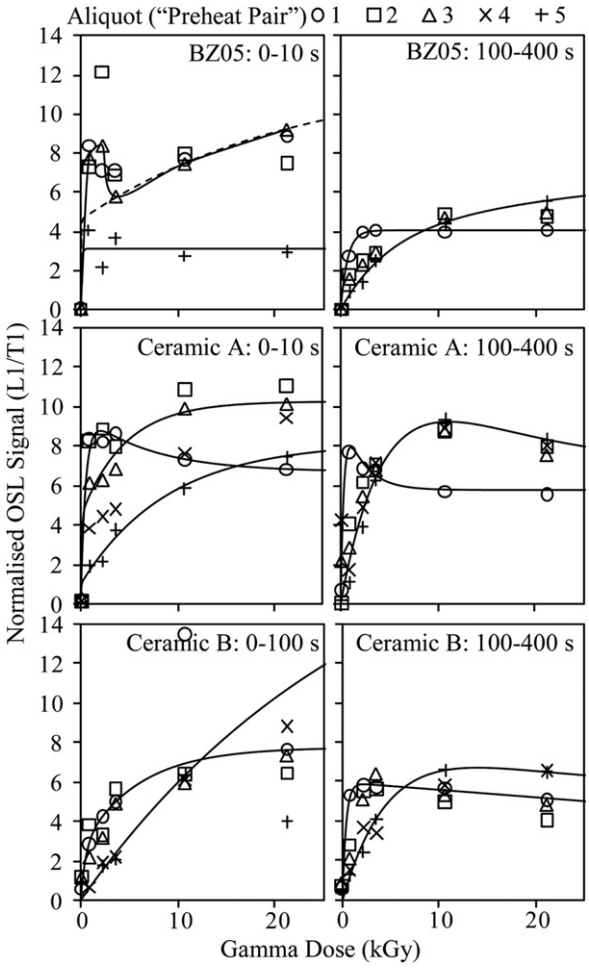

Fig. 5. Gamma dose response of OSL signals (L1; Table 1, Step iii), measured following a range of preheats of different severities (Aliquot "Preheat Pair" 1–5, Table 1). The OSL signals were transformed from LMOSL measurements and integrated over different periods of optical stimulation (0–10 s, 0–100 s, 100–400 s). Gamma dose response is normalised to the OSL response to a subsequent beta test dose (T1; Table 1, Step viii). Curves fitted to selected datasets are single and double saturating exponentials, plus one spline following the response of BZ05: 0–10 s, aliquot 3.

rate to the slower TTOSL signals and, for the less severe preheats applied to Aliquot 1, at a similar rate to the slower signals in the test dose responses. The faster TTOSL signals increased with dose at a more constant rate across the whole range of doses; particularly for the severe preheat and after allowing for inter-aliquot variations in sensitivity.

The dose response characteristics of test dose-normalised signals (Figs. 5 and 6) were commonly well approximated by two saturating exponential components ($\{A; B\}_1$ and $\{A; B\}_2$ in Eqn. (1). It was often the case that one component saturated at low doses and/or exhibited a saturating negative trend (small B value and/or negative A value). This was more common in OSL than TTOSL signals, and in many cases the contribution of such components was reduced following higher preheats.

For sample BZ05, the normalised dose response of faster OSL signals following lower preheats (Fig. 5. BZ05: 0–10 s) increased rapidly and then diminished, followed by more gradual increases with dose above 5 kGy. Use of the regenerative beta response to predict the previous gamma dose produced overestimates of 7% above 5 kGy (Table 2). Use of slower OSL and TTOSL signals from BZ05 enabled prediction of the given gamma doses throughout the range of doses analysed, within deviations of 3–4%. However, predictions for the ceramic samples were less successful: residuals were larger and the useful dose range was limited.

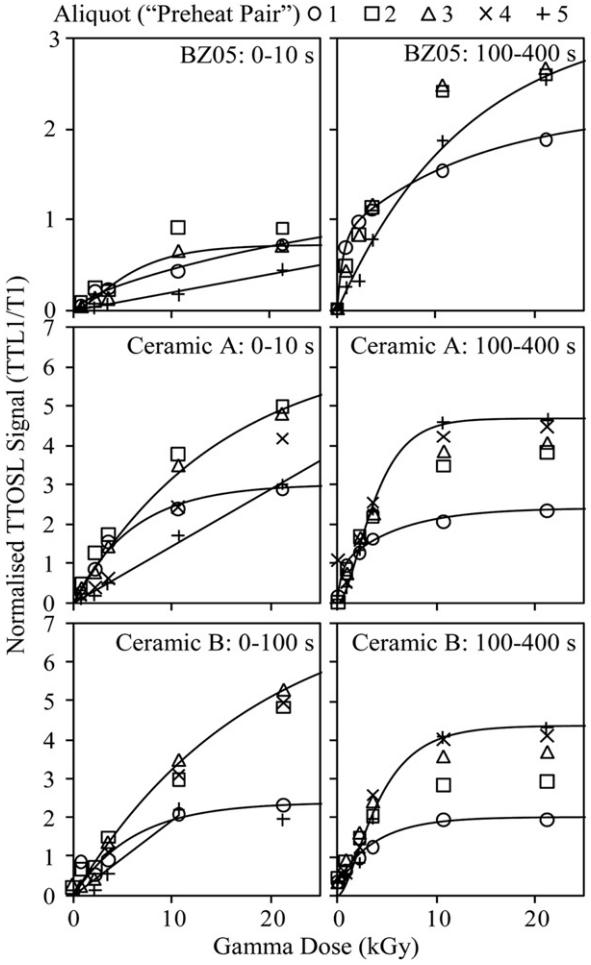

Fig. 6. Gamma dose response of TTOSL signals made following a range of preheats of different severities (TTL1; Table 1, Step v): and see Fig. 3 caption. Curves fitted to selected datasets are single and double saturating exponentials, but note linear regressions for data recoded from each sample using the shorter signal integral period (0–10 s or 0–100 s) and the most severe preheat (Table 1, aliquot 5).

Table 2
Difference between given gamma dose and that predicted using the response of the samples to subsequent beta irradiation, for selected signals and preheat combinations. The mean and standard deviation of the differences were calculated for dose intervals selected to illustrate the most useful range for a given signal and preheat combination.

Sample			Form of Fit[a]		Predicted - Given Gamma Dose		
Signal type	Integral period (s)	Aliquot (Preheat)	γ Dose Response	β Dose Response	Mean (%)	s.d.	In Interval (kGy)
BZ05							
OSL	1–10	3	4cSE	4cSE	7	1	5–30
TTOSL	1–10	5	Linear	Linear	−23		0–30
OSL	100–400	5	4cSE	4cSE	0	4	1–30
TTOSL	100–400	5	2cSE	2cSE	−2	3	1–30
Ceramic A							
OSL	1–10	5	4cSE	4cSE	14	5	1–20
TTOSL	1–10	5	Linear	Linear	−15		0–30
OSL	100–400	5	4cSE	2cSE	−24	4	1–10
TTOSL	100–400	5	4cSE	4cSE	−5	14	1–15
Ceramic B							
OSL	1–100	5	2cSE	4cSE	33	11	1–10
TTOSL	1–100	5	Linear	Linear	−17	[b]	0–10
OSL	100–400	5	4cSE	2cSE	20	1	1–10
TTOSL	100–400	5	4cSE	4cSE	−9	3	3–15

[a] 2/4cSE = two/four component saturating exponential.
[b] Subsample F excluded from fit (see Fig. 6).

Following a 300 °C preheat, faster TTOSL signals produced linear dose responses for all samples. The linear trend continued up to 20 kGy gamma (Fig. 6) and 30 kGy of beta irradiation for samples BZ05 and Ceramic A. For Ceramic B it was evident for the first 10 kGy, but was followed by very different rates of saturation in the gamma and beta responses. Predictions based on these linear dose responses underestimated the given gamma doses by 15–23% (Table 2).

4. Discussion

OSL signals follow exponential decays and so exhibit a large range of magnitudes during a single measurement. Non-linearity in photomultiplier response exceeds approximately 1% for count rates above 10^6 cps (Hamamatsu, 2006, Figs. 6–8). Correction for pulse overlapping may extend effective linearity to 5×10^7 cps, but requires accurate knowledge of the photomultiplier's pulse-pair resolution. In the present study linear modulation of the stimulation power during OSL measurement was instead used to reduce the dynamic range of the signal to be detected, without the reduction in detection sensitivity that would accompany the use of masks or neutral density filters. This facilitated the measurement of different signals with very high and very low sensitivities to dose and/or detrapping by 470 nm photons, with the same experimental configuration.

Increase in LMOSL background as a power function of stimulation power (Fig. 1), and the similar results from empty and loaded cups, indicate that the background above dark count relates to breakthrough of stimulating light and/or anti-stokes fluorescence of the detection filters, rather than coming from the sample material itself. However, this background was less than 1% of the majority of signals measured in the present study (Fig. 2), so its exact evaluation made little difference to the dosimetric results. After subtraction of the instrumental background, transformation of the LMOSL signals into OSL-form permitted the conventional subtraction of slowly decaying signals from the dosimetric response.

Faster OSL signals increased rapidly at low doses but then saturated. Variation of the saturated signal levels with sensitivity confirms the need for dose normalization to correct for differences in recombination efficiency and hence compare precisely

between results from different aliquots (Fig. 4). TTOSL responses continued increasing to higher doses than OSL, but also varied with OSL sensitivity. In the present study the OSL test dose response was more directly relatable to the TTOSL measurement than to the OSL measurement. This is because of possible changes in recombination efficiency through the measurement of the large OSL signals from the large beta or gamma doses (Table 1, Steps iii, xii), and during the TTOSL preheat (Table 1, Steps iv, xiii), which was 20 °C higher than that for the preceding OSL measurement. Such sensitivity changes could artificially alter the size of T# relative to L#, and hence alter normalised dose response characteristics. Changes in their magnitude before and after the 500 °C anneal (Table 1, Step ix) may have affected the accuracy of the retrospective dose evaluations, but these mechanisms do not appear to significantly affect the basic form of the dose response: similar patterns of normalised dose response were obtained before and after the 500 °C anneal, and negative components were apparent in the dose response of non-normalised faster OSL signals (Fig. 4, Aliquot 1, 0–10 s, L1, L2).

High preheats were observed to reduce the slower signals more than the faster ones, indicating that some slower signals relate to different, less thermally stable trap types. LMOSL curves and non-normalised signal integrals (Figs. 2 and 4) indicate how the slower OSL signals continue increasing to higher doses than the faster OSL signals. However, when subject to lower preheats the test dose responses of the slower signals increased as a function of the previous beta or gamma dose, and increased more strongly from one cycle to the next. This indicates the presence of residual or recuperated signals in the test dose responses, which increase monotonically with dose and from measurement cycle to measurement cycle. Such signals appear to contribute to the negative components observed at high doses, in the normalised dose responses of the slower signals, by artificially reducing the ratio L#/T#.

The peak observed in the faster OSL signals from BZ05 (0–10 s, Fig. 5) may relate to problems encountered in attaining "natural" signal levels in the regenerated dose responses of geological quartz samples (Burbidge et al., 2009). It was removed by preheating at 300 °C for 30 s and so appears to derive from the "325 °C TL" region, from which the majority of the OSL signal conventionally employed in dating and dosimetry with quartz arises. The peak was apparent between 1 and 5 kGy for both bulk-gamma and on-disk beta irradiations (Fig. 4). Since the gamma dose rate used in the present study was approximately 17 times higher than the beta dose rate, this effect appears to be a function of dose and not dose rate. Increased recuperation observed in the slower signals indicates the filling of deep traps/centres, not emptied by OSL measurement, preheating, or annealing to 500 °C. This might produce changes in trapping probability which, unlike recombination efficiency, would not be well monitored by the test doses.

Increases in signal with dose were strongest for faster TTOSL signals measured following higher preheats. Approximately proportional increases up to 30 kGy were obtained from samples BZ05 and Ceramic A, when they were preheated to 300 °C after irradiation. A larger signal integral was used for Ceramic B, to reduce statistical scatter from very low signal levels in the first measurement cycle (Fig. 2): this may have limited the useful dose range of measurements on this sample. Underestimates of around 20% in the prediction of the given gamma doses using regressions to the linear trends, might relate to uncorrected changes in sensitivity to dose or to signal instability: the delay between gamma irradiation and measurement was longer than that for beta irradiation. However, the linear nature of this signal's dose response makes it an interesting prospect for future investigations of kGy dosimetry using quartz, and indicates that it may continue to increase to higher doses.

5. Conclusions

LMOSL provides a convenient means to limit count rates when measuring bright or high-dose samples, while still enabling small signals to be measured. OSL instrumental background consists of a constant dark count, plus breakthrough/filter fluorescence as a power function of stimulation intensity.

Luminescence signals that exhibited increases with dose to at least 30 kGy were identified in the quartz samples analysed. Faster OSL signals exhibited dose response characteristics that were highly preheat dependant and variable in form between samples. Slower OSL and TTOSL signals were affected by residuals or recuperation. A major challenge, in the development of measurement protocols for multi-kGy retrospective dosimetry using quartz, appears to relate to variations in the contribution of rapidly saturating and non-monotonic components in the response of signals to increasing dose. Following severe preheats, faster TTOSL signals exhibited approximately linear growth to tens of kGy and enabled retrospective dose evaluation for each sample with an accuracy of 15–23%. This first order approximation is already sufficient to provide estimates for severity of radiation exposure. Improvements in accuracy and precision of the protocol applied in the present study are dependent on the appropriateness of using a test dose correction to normalise the dose responses.

The present study has identified certain elements of OSL and TTOSL signals that can be used to retrospectively evaluate doses of tens of kGy: an order of magnitude beyond the range traditionally considered possible using quartz and other silicates.

Acknowledgements

This work was funded by the FCT through the project PTDC/HIS-HEC/101756/2008-RADIART. The authors thank M. A. A. Pinto de Matos and A. Pais (Museu Nacional do Azulejo) for the ceramics and L. Rebêlo (LNEG) for BZ05, sampled with support of the Instituto Português de Apoio ao Desenvolvimento.

References

Aitken, M.J., 1985. Thermoluminescence Dating. Academic Press.
Bulur, E., 2000. A simple transformation for converting CW-OSL curves to LM-OSL curves. Radiat. Meas. 32, 141–145.
Burbidge, C., Dias, M., Prudêncio, M., Rebêlo, L., Cardoso, G., Brito, P., 2009. Internal α activity: localisation, compositional associations and effects on OSL signals in quartz approaching β saturation. Radiat. Meas. 44, 494–500.
D' Oca, M., Bartolotta, A., Cammilleri, M., Brai, M., Marrale, M., Triolo, A., Parlato, A., 2007. Qualitative and quantitative thermoluminescence analysis on irradiated oregano. Food Control 18, 996–1001.
Hamamatsu, 2006. Photomultiplier Tubes: Basics and Applications, third ed. Hamamatsu Photonics K.K., Electron Tube Division.
Han, Z., Li, S., Tso, M., 2001. TL dating of granitic quartz using an additive alpha dose method. Quat. Sci. Rev. 20, 907–911.
Li, B., Li, S., 2006. Studies of thermal stability of charges associated with thermal transfer of OSL from quartz. J. Phys. D: Appl. Phys. 39, 2941–2949.
Portugal, L., Cardoso, J., Oliveira, C., 2010. Monte Carlo validation of the irradiator parameters of the Portuguese gamma irradiation facility after its replenishment. Appl. Radiat. Isot 68, 190–195.
Rink, W., 1994. Billion-year age dependence of luminescence in granitic quartz. Radiat. Meas. 23, 419–422.
Sanderson, D., Slater, C., Cairns, K., 1989. Detection of irradiated food. Nature 340, 23–24.
Singarayer, J.S., Bailey, R.M., 2003. Further investigations of the quartz optically stimulated luminescence components using linear modulation. Radiat. Meas. 37, 451–458.
Spooner, N.A., Questiaux, D.G., 2000. Kinetics of red, blue and UV thermoluminescence and optically stimulated luminescence from quartz. Radiat. Meas. 32, 659–666.
Storm, E., Israel, H.I., 1970. Photon cross sections from 1 keV to 100 MeV for elements Z = 1 to Z = 100. Nucl. Data Tab A7, 565–681.
Tsukamoto, S., Duller, G., Wintle, A., 2008. Characteristics of thermally transferred optically stimulated luminescence (TT-OSL) in quartz and its potential for dating sediments. Radiat. Meas. 43, 1204–1218.